CSIRO PUBLISHING

www.publish.csiro.au/journals/mfr *Marine and Freshwater Research*, 2005, **56**, 549–560

Recent growth rate of larval pilchards *Sardinops sagax* in relation to their stable isotope composition, in an upwelling zone of the East Australian Current

Shinji Uehara[A,B], *Augy Syahailatua*[A] *and Iain M. Suthers*[A,C]

[A]School of Biological, Earth and Environmental Sciences, University of New South Wales, Sydney, NSW 2052, Australia.
[B]Kuroshio Research Division, National Research Institute of Fisheries Science, 6-1-21 Sanbashidori, Kochi 780-8010, Japan.
[C]Corresponding author. Email: i.suthers@unsw.edu.au

Abstract. The recent growth rate and stable isotope composition of larval pilchards, (*Sardinops sagax*, 6–29 mm standard length), captured in surface and near-surface waters, were examined in coastal upwelling and non-upwelling regions of the East Australian Current over two cruises during the austral summer of 1998/1999. Compared to the non-upwelled regions, larvae were larger in the upwelling regions, and yet the back-calculated recent growth over 2 days before capture was significantly less on both cruises. This surprising result is consistent with slower larval growth of this species near coastal Japan and California, where strong year classes may form in offshore waters. δ^{15}N ratios were significantly correlated with larval length, indicating ontogeny in their diet. In November, slower growers in upwelled waters were enriched in δ^{15}N and depleted in δ^{13}C, consistent with expected ratios from diets derived from deeper water. The pilchard's early life history off eastern Australia is proposed and compared with that off eastern Japan.

Extra keywords: age, back-calculation, condition, daily growth increments, fish larvae, Kuroshio, recent otolith growth, sagitta, Tasman Front, western boundary current.

Introduction

Year class strengths of planktivores such as herring, pilchard or anchovy are frequently stimulated by coastal upwelling during the spawning season, in association with favourable winds (Cury and Roy 1989; Ware and Thomson 1991). The actual process that enhances recruitment is unclear, and can vary non-linearly with the strength of winds (Cury and Roy 1989) and with the locality. Response to upwelling is season-specific for sardine (*Sardina pilchardus*) and horse mackerel (*Trachurus trachurus*) off Portugal, having a negative influence during winter spawning, but positive influence during the spring-summer juvenile phase (Santos *et al*. 2001). It would appear the response to nutrient supply is species- and location-specific.

The Pacific sardine, or pilchard *Sardinops sagax* is a cosmopolitan species with important fisheries in Australia, Japan, South Africa, Chile and California. As a consequence, their larval ecology has been studied and their growth rates in particular, well researched (overview in Gaughan *et al*. 2001). Pilchards were not appreciated as being abundant off eastern Australia, until widespread deaths of pilchards were observed in 1995 and again in 1998 (Griffin *et al*. 1997; Gaughan *et al*. 2001). Pilchards are important for the coastal ecosystem, as the effects of this die-off were severe for local marine birds (Bunce and Norman 2000; Dann *et al*. 2000), and for the west coast fishery. Nevertheless, our knowledge of the pilchard on the east coast is very limited, but as the genus is now considered to be monospecific (Grant *et al*. 1998), there are useful parallels with *Sardinops* studies off Western Australia (Gaughan *et al*. 2001), California (Logerwell and Smith 2001), and Japan (Watanabe and Kuroki 1997).

The slower growth parameters of Western Australia larval and adult pilchard were argued to be the result of nutrient limitation in the characteristically oligotrophic waters, compared with elsewhere in the world (Gaughan *et al*. 2001). If growth is actually limited by nutrient availability, then the source of the assimilated nutrients supporting either faster or slower larval growth could be identified by their stable isotope composition. Stable isotope analysis (SIA) of carbon and nitrogen (δ^{13}C and δ^{15}N) in the tissues of planktivorous fish has proved useful in identifying the contribution of upwelled nutrients, which have distinctive stable isotope signatures (Gaston and Suthers 2004). Stable isotope analysis has the advantage of indicating the C and N that is actually assimilated compared to traditional gut content analyses. The proportion of the rarer, heavier, stable isotope is assessed by comparison to an international standard, and expressed as parts per thousand (‰).

© CSIRO 2005 10.1071/MF04221 1323-1650/05/050549

There are very few studies of stable isotopes and larval fish, partly because of the amount of tissue necessary (0.5–1 mg dry weight, equivalent to nearly 10 individual larvae). The stable isotope composition of larval fish varies with size, from hatch (containing the maternal contribution) to transformation when the diets may suddenly change (Lindsay *et al*. 1998; Vander Zanden *et al*. 1998). Similar changes in composition are observed at settlement to seagrass beds in juvenile red drum (Herzka and Holt 2000; Herzka *et al*. 2001). The SIA of larvae reveals rapid changes, over 2–3 days at 18°C as a result of both tissue turnover and particularly to growth (Bosley *et al*. 2002). The change in stable isotope composition of fish larvae thus approximates the time scale of response of daily growth from otolith microstructure. The recent daily growth increments of the otolith provide a robust method of assessing the response of growth rate to a variety of local environmental conditions (summarised in Suthers 1998). In particular, the daily growth increments of pilchards are amenable to this analysis, and larval Atlantic menhaden were found to respond to a stress factor within 2 days (Maillet and Checkley 1990). The relationship between larval growth and stable isotope composition was first documented for a larval gadoid (*Macruronus novaezelandiae*, Thresher *et al*. 1989, 1992). Small larvae retained near the spawning area off western Tasmania had faster growth compared with similarly small larvae that were advected south (Thresher *et al*. 1989). The faster growing larvae near the spawning area had a distinctively depleted $\delta^{13}C$ composition from their tintinnid diet, which was derived from the offshore advection of terrestrially depleted seagrass detritus (Thresher *et al*. 1992). No other study has simultaneously compared larval growth rates and the stable isotope composition.

The East Australian Current (EAC) transports clear oligotrophic waters from the Coral Sea poleward, but can stimulate a variety of upwellings at the separation point off northern New South Wales (NSW), where it forms the Tasman Front. There should be dramatic influence on larval growth and their composition, but no study has made the simultaneous comparison of growth rates and stable isotope composition. Therefore, our first aim was to test if recent otolith growth (ROG) of larval pilchards was significantly different between pre-upwelled conditions of the EAC and topographically induced upwelling conditions. Our second aim was to compare the larval ROG with the corresponding stable isotope composition, to determine if the source of C and N between faster and slower growing larval pilchards was different. We compare our findings with other larval pilchard studies to infer the early life history of pilchards off eastern Australia.

Materials and methods

Study area

The continental shelf bounded by the 200 m isobath off northern NSW, narrows from 33 km wide off the town of Urunga (referred to herein as Region 1), to just 16 km wide off Smoky Cape (Region 2), in a distance of 43 km. Smoky Cape is located approximately 430 km north of Sydney (Fig. 1). In response, the poleward EAC accelerates through this region, forcing deep water up into near-surface coastal regions, 100 km south of Smoky Cape at Diamond Head (Region 4) and Cape Hawke (Region 5, Cresswell 1994; Roughan and Middleton 2002). Here, the continental shelf extends to 22 km wide at Point Plomer (Region 3), to 32 km wide at Diamond Head (Region 4) and 47 km wide off Cape Hawke (Region 5, Fig. 1). While the currents offshore of 100 m were $>1\ m\ s^{-1}$, at the 50 m station where we collected larvae, currents were usually south and $<0.3\ m\ s^{-1}$, such that the distance between Regions 1 and 4 (120 km) was greater than any drift distance during our 2-day growth back-calculation (Fig. 1). Upwelling in the region has been well studied (Cresswell 1994; Oke and Middleton 2000, 2001; Roughan and Middleton 2002), and has a significant effect on phytoplankton and algal blooms (Dela Cruz *et al*. 2002, 2003).

Plankton sampling and design

Two summer cruises by the Research Vessel Franklin were undertaken in November 1998 and January 1999, taking replicated samples near the 50 m isobath off Regions 1, 3, and 4 in late November 1998, and off Regions 1, 2, 3, 4, and 5 in January 1999 (Fig. 1). Sampling was also conducted at the 100 m isobath (Syahailatua 2004), but few pilchard larvae were caught at the 100 m station in January and were not further analysed. Larval fish were collected at night by simultaneous tows with a neuston net (75 × 75 cm, 500 μm mesh) and a subsurface opening and closing net ('EZNET', 1 m^2 mouth opening, 500 μm mesh) at 10–20 m from the surface at the 50 m station. The EZNET was also deployed over deeper depth strata but few pilchard larvae were obtained in these and were not further analysed. All nets had a flow meter to calculate volume filtered. Larvae from the two gear types were combined for the present study to attain sample size. Replicated tows were conducted with the neuston net and in part with the multiple opening and closing net and were combined for each night at each region (Table 1). Larvae were compared from Regions 1 to 3 (pre-upwelled waters of the EAC) with those from the topographically induced upwelled waters (Regions 4 and 5). Similar events were observed on both cruises.

During the cruise, a calibrated thermosalinograph and a calibrated fluorometer operated continuously. At each station a depth profile was made using a Neil-Brown conductivity-temperature-depth meter. Inside the surface and subsurface nets, a 20 cm diameter 100 μm mesh net was mounted, to obtain microzooplankton abundance.

Plankton samples were immediately preserved in 5% buffered formalin (to preserve the otoliths, samples were buffered using sodium carbonate which caused some bleaching of the melanophore pattern after 2–3 months). Back at the laboratory the larvae were sorted out from the plankton, using the identification key of Neira *et al*. (1998), and larvae were stored in 95% ethanol until otolith analysis. Too few larvae were sampled in January at Regions 2 and 3 for otolith analysis. All larvae were measured for standard length (SL, up to a maximum of 100 larvae per sample, Table 1), using image analysis. The microzooplankton samples were gently rinsed with seawater through a 90 μm mesh sieve and concentrated to 0.1 L, and zooplankton counts were made on two replicate subsamples and converted to numbers L^{-1}.

Otolith analyses

Between eight and 10 larvae per sample were selected for otolith analyses (in proportion to the size range, Table 1). Using a dissecting microscope and polarised light we removed both sagittae and mounted them onto separate glass slides with nail polish. The otolith radii and increment width series along the longest axis were measured using a compound microscope (64 × oil immersion lens) and by image analysis.

Daily increment counts of all fish were checked by independent counts from a random, blind-labelled subsample ($n = 27$) by a second

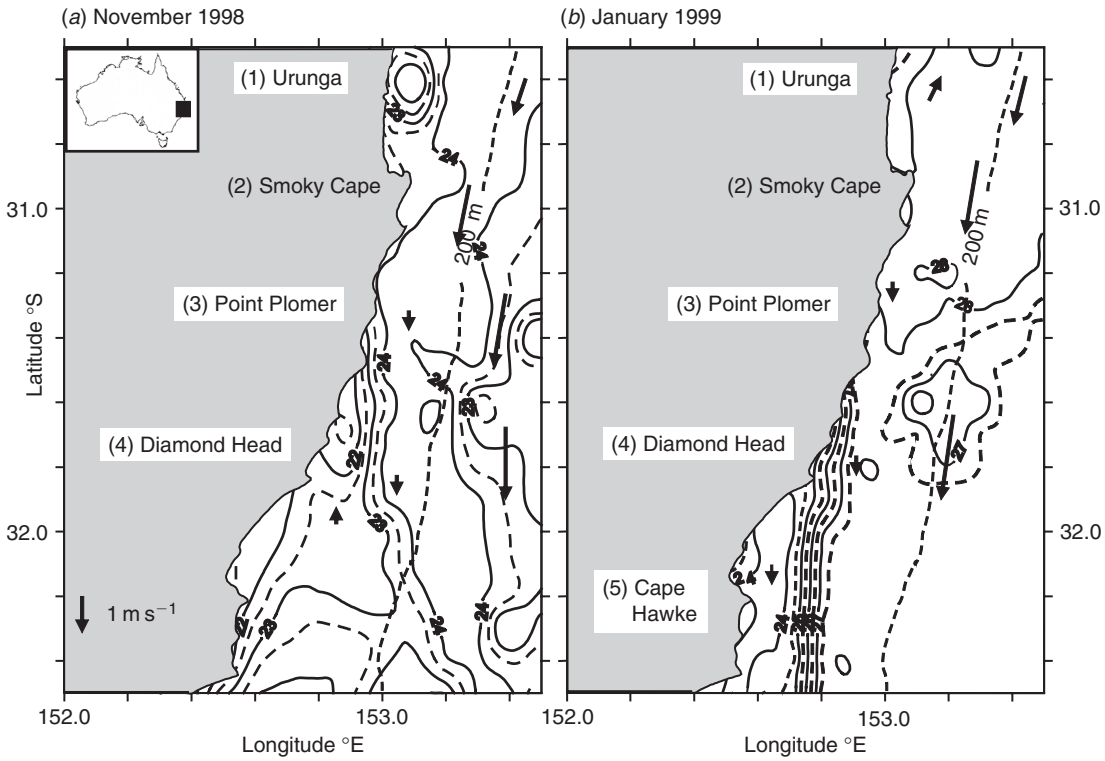

Fig. 1. Contours of sea surface temperature (SST), derived from NOAA 14 satellite images of the northern NSW coast on (*a*) 21 November 1998, and (*b*) 19 January 1999. The highlighted sampling regions were subsampled for age and stable isotope analyses. Representative vectors show currents measured underway using the shipboard acoustic Doppler current profiler.

reader. Counts were highly correlated ($r = 0.92$), with a mean difference of 0.7 (range of differences from −3 to +1). Since the initial daily growth ring is deposited at 2–3 days after hatching (Hayashi *et al*. 1989), we added 2 days to the total increment count, to estimate the post hatching age of pilchard larvae.

Back-calculation of length at 2, 4, 6 and 8 days pre-capture was calculated using the non-linear method of Watanabe and Kuroki (1997), which incorporates the biological intercept method (Campana and Jones 1992, Eqn 27). Daily increment formation in this species was demonstrated by Hayashi *et al*. (1989), and was re-examined in the current study by marginal increment formation (see Results). Following the rationale of Watanabe and Kuroki (1997), we used the preserved length = 5.0 mm at first feeding when daily increments begin to be deposited at age 3 days (Hayashi *et al*. 1989). We then calculated the change in length during Days 1 & 2 precapture, Days 3 & 4, Days 5 & 6 and Days 7 & 8. We did not back-calculate to within six increments of the first feeding ring (8 days old), to avoid back-calculation to the size range less than we caught.

We initially used the Campana and Jones (1992, Eqn 27) biological intercept method of back-calculation, as the length–radius (L–R) relationship appeared linear, with minimal improvement in the R^2 statistic for various non-linear fits (power curve, L–ln(R), or ln(L)–ln(R)). However, R^2 is insensitive to departures from linearity in small and large fish, as revealed by inspection of the residuals plot. Watanabe and Kuroki (1997) use a power curve $L = a \times R^b$ to back-calculate size, incorporating the biological intercept concept, by solving the parameters a and b for each larva for two points in time: at hatch and at capture. Watanabe and Kuroki (1997) set the size at hatch (actually the first feeding check, for pilchard larvae caught in a plankton net and preserved in formalin) at 5 mm, and used each individual's hatch check diameter. Solving for a and b gives:

$$a = L_h/(R_h^b) \quad (1)$$

$$b = \ln(L_h/L_c)/\ln(R_h/R_c) \quad (2)$$

where L_h is the size at hatch (set at 5 mm), R_h is the hatch check radius (or in the case of *S. sagax* is the first feeding check), L_c is the length at capture and R_c is the otolith radius at capture. Using the individually determined parameters a and b, the length at various radii (ages) could then be back-calculated. Interestingly, an almost identical back-calculation was obtained using the sample level estimates (i.e. not individual level) of the modified Fry equation (Vigliola *et al*. 2000).

Linear growth models and Laird–Gompertz growth models (only November 1998 data) were fitted to the length on age data. We used the following form of the Laird–Gompertz (Eqn 15, Campana and Jones 1992):

$$L_t = L_\infty \exp[-\exp(-G\{\text{age} - X_0\})], \quad (3)$$

where L_∞ is the asymptotic length, G is the instantaneous rate of growth at age X_0 and X_0 is the inflection point of the curve. Laird–Gompertz growth functions were fitted iteratively to the length-age data for comparison of parameter values with published reports. The back-calculated recent growth (RG) was compared among regions by ANCOVA and tested with temperature and prey abundance by linear regression. Length–frequency distributions off each region, with each gear type (neuston or EZNET) were compared by a pairwise Kolmogorov Smirnov (KS) test, with an adjusted P-value of significance set at $P = 0.01$. Larval density (number per 100 m^3) and stable isotope

Table 1. Summary of samples collected on the two cruises showing the date in November 1998 and January 1999, local time of collection, the type and depth of net (0–1 m, neuston net; 10–20 m, EZ subsurface net) and total no. of larvae collected

Region	Date	Time	Net	Total	Morphology		Otolith		SIA
					n	SL range	*n*	SL range	*n*
1) Urunga	21 Nov	23:34	0–1	40	40	9.2–16.1	9	11.4–15.0	9
		23:47	0–1	18	16	10.7–17.0	9	12.5–17.0	9
	22 Nov	3:09	0–1	2	2	11.2–13.7	2	11.2–13.7	2
		3:26	0–1	4	4	8.4–11.8	4	8.4–11.8	3
	23 Nov	1:30	10–20	15	15	7.5–17.0	14	7.5–17.0	14
3) Point Plomer	23 Nov	21:38	0–1	12	12	8.3–16.1	9	9.5–16.1	–
	23 Nov	21:38	10–20	68	66	6.8–16.4	9	10.4–16.1	9
	24 Nov	3:40	10–20	59	47	6.8–15.8	9	11.3–15.8	9
4) Diamond Head	24 Nov	23:44	0–1	80	77	13.6–18.5	9	16.7–18.3	10
		23:58	0–1	199	199	9.2–20.3	9	16.3–18.4	9
	24 Nov	23:25	10–20	98	81	8.5–14.3	9	9.3–14.3	9
	25 Nov	3:00	10–20	152	103	8.6–17.6	9	10.1–15.9	–
Subtotal				2230	1116		156		83
1) Urunga	21 Jan	22:25	0–1	35	26	8.6–13.5	22	8.6–13.5	10
	22 Jan	3:43	0–1	2	2	10.1–12.9	2	10.8–12.9	–
	21 Jan	22:00	10–20	3	3	5.0–9.8	–	–	–
	22 Jan	3:30	10–20	20	14	7.8–11.2	18	7.8–11.2	20
4) Diamond Head	25 Jan	0:55	0–1	7	6	9.5–15.1	6	9.5–15.1	6
	25 Jan	1:07	0–1	4	4	11.8–15.9	4	11.8–15.9	4
	24 Jan	21:00	10–20	16	13	7.3–14.9	13	7.3–14.9	16
	25 Jan	1:00	10–20	18	18	9.3–15.7	17	9.3–15.7	18
5) Cape Hawke	25 Jan	21:50	0–1	2	2	12.7–15.5	2	12.7–15.5	2
	26 Jan	2:25	0–1	2	2	13.6–16.6	2	13.6–16.6	2
	26 Jan	2:32	0–1	2	2	13.6–17.9	2	13.6–17.9	2
	28 Jan	21:54	0–1	7	7	12.9–16.7	7	12.9–16.7	7
	28 Jan	22:16	0–1	12	12	8.2–15.9	12	8.2–15.9	7
	25 Jan	21:43	10–20	6	5	10.9–14.2	6	10.9–14.2	6
	26 Jan	2:30	10–20	7	6	10.0–14.0	6	10.4–13.2	7
Subtotal				143	122		119		107

n, no. of individuals; SIA, no. used for stable isotope analysis; SL, standard length (mm).

Table 2. Parameter estimates for the fitted Laird–Gompertz growth function for *S. sagax* from eastern Australia in November 1998, shown in Fig. 5 ($n = 215$, $R^2 = 0.65$)

Parameter	Estimate (s.e.)	95% CI
L_∞	23.936 (3.713)	16.6–31.278
G	0.092 (0.027)	0.04–0.15
X_0	8.140 (1.417)	5.3–10.9

L_∞, Asymptotic length; G, instantaneous rate of growth at age X_0; X_0, is the inflection point (age) of the curve.

ratios were tested for homogeneity by Cochrans test and compared among regions by ANOVA.

Stable isotope analyses

The larval body remaining from the otolith dissection (i.e. less the head) was then freeze-dried to a constant weight cut up into small pieces and approximately 1.5–1.7 mg of the tail musculature was sealed into foil capsules. Stable isotope analysis on each capsule was performed at the CSIRO Land and Water Adelaide Laboratory on an automated nitrogen carbon analysis–mass spectrometer (Sercon Australia Pty Ltd, Adelaide). Capsules were combusted and the reaction products separated by gas chromatography to give pulses of pure CO_2 and N_2 for analysis of total C and N, and $\delta^{13}C$ and $\delta^{15}N$. Isotope values were expressed in del (δ) notation, $\delta^{13}C$ and $\delta^{15}N$, relative to standards (glycine for carbon and ethylenediaminetetraacetic acid (EDTA) for nitrogen) that had been calibrated against international standards (Gaston and Suthers 2004). The precision in $\delta^{13}C$ and $\delta^{15}N$ analyses was $\pm 0.2‰$.

Results

Oceanographic conditions and larval distribution

Synoptic sea surface temperature images on both cruises revealed a front and separation of the EAC from the coast, near Point Plomer (Fig. 1, Roughan and Middleton 2002). Consequently a strong temperature gradient was evident off Diamond Head, with a horizontal difference of 1–2°C in November and 3–4°C in January. At the 50 m station, cooler water was evident at Diamond Head, with an elevation of isotherms by 40 m (Fig. 2). Maximum currents were observed beyond the 100 m isobath off Smoky Cape of >1.5 m s^{-1}, but were <0.5 m s^{-1} near the 50 m station and sometimes even reversed to the north, off Diamond Head (Fig. 1, Roughan and Middleton 2002).

Pilchard larvae were 10-fold more abundant in November than later in summer during January (Fig. 3*a*,*b*). Overall,

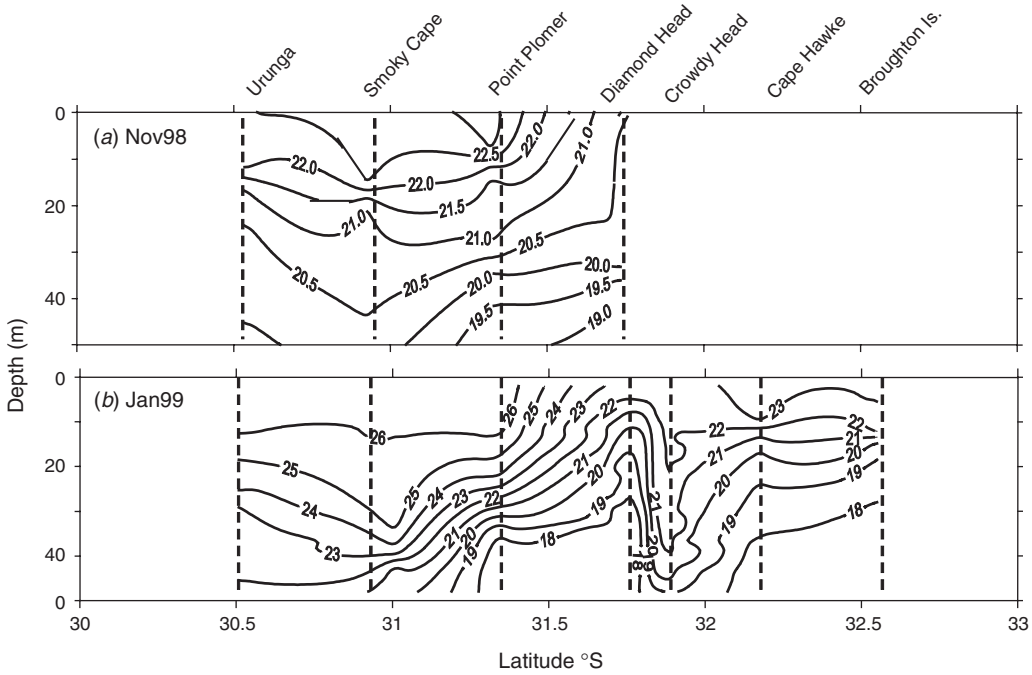

Fig. 2. Alongshore temperature profiles derived from conductivity–temperature–depth (CTD) casts at the 50 m station during (*a*) November 1998 and (*b*) January 1999. Upwelling off Diamond Head is evident by the uplifted isotherms.

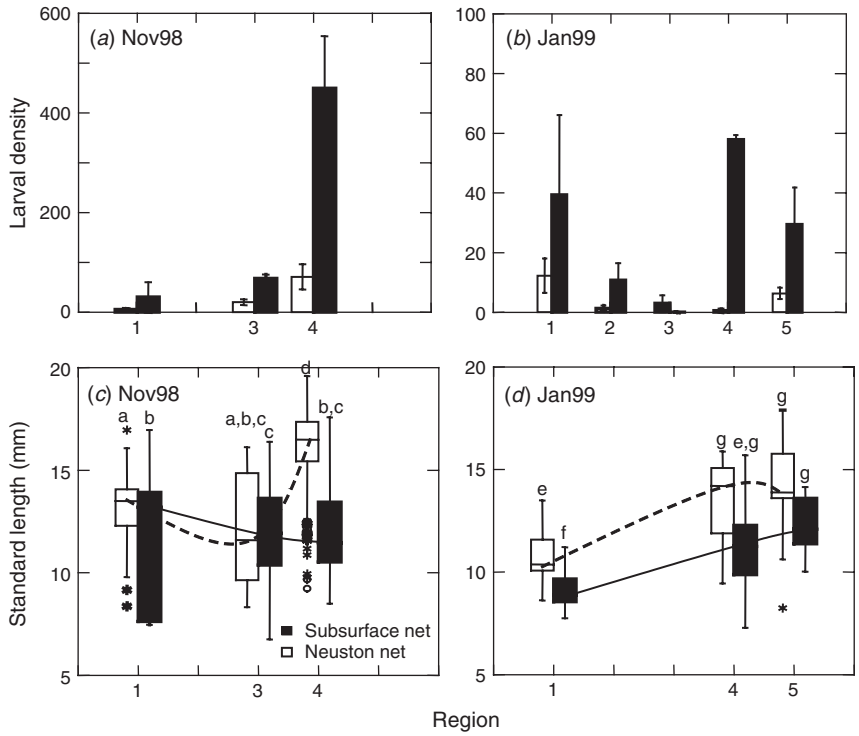

Fig. 3. Larval density of pilchards (no. per 100 m^3) across regions in (*a*) November 1998 and (*b*) January 1999, and corresponding box and whisker plots of the length–frequency distribution of larval pilchards (*c*) November 1998 and (*d*) January 1999. Significant differences in the cumulative length–frequency distribution shown in (*c*), (*d*) by a Kolmogorov Smirnov test ($P < 0.01$) are identified with a different letter. Outliers are shown by an asterisk.

2628 pilchard larvae were collected in November 1998 (over all nets and regions, approximately 24 larvae 100 m^{-3}) and 143 larvae collected in January 1999 (overall approximately two larvae 100 m^{-3}). During November we observed similar abundances in the neuston and subsurface nets, but comparisons across regions by ANOVA were confounded by non-homogeneity of variance. During November the average log concentration of larval pilchards was three- to 10-fold greater in the upwelling regions off Region 4 (Diamond Head) compared to Region 1 (Fig. 3*a*), and in January there was no consistent alongshore pattern (Fig. 3*b*).

The SL of larvae was unimodally distributed between 5 and 25 mm, with the average SL in November (14.8 mm, s.e. = 0.1) greater than in January (11.7 mm, s.e. = 0.2). There were no consistent trends in length between sampling gear (Fig. 3*c*,*d*), with the exception of the subsurface net in November (Fig. 3*c*). In both months the length distribution from Regions 1 and 3 to 4 or 5 was significantly shifted to the larger sizes (Fig. 3*c*,*d*, KS test, $P < 0.01$, except the subsurface net, November).

Otolith microstructure and growth

The pilchard otoliths had an average hatch check diameter of 11.6 μm, with two to four faint perinuclear increments before an established and definite pattern was evident (Fig. 4). The average proportion of the marginal increment was almost 100% of the previous increment by early in the evening (20:00–21:00 hours, S. Uehara, unpublished data). This proportion declined during the night such that around 02:00 the average proportion was approximately 40%, consistent with daily increment formation.

A linear model adequately described the relationship between size and age, with a similar R^2 statistic between months, and a similar corrected R^2 statistic for the Laird–Gompertz model, calculated for November data only (Fig. 5, Table 2). There were insufficient older larvae in January to determine a non-linear fit. The linear growth curves were:

$$\text{November 1998, SL} = 4.224 + 0.625 \times \text{age} \quad (R^2 = 0.64, n = 215) \text{ and}$$

$$\text{January 1999, SL} = 0.551 + 0.976 \times \text{age} \quad (R^2 = 0.66, n = 110).$$

The slope of the linear regression for November (0.63 and 0.98 for January, Fig. 5) is similar to the range of daily growth estimated for larvae between 5 and 25 days old, from the Laird–Gompertz model for November (average: 0.64 mm day^{-1}, range: 0.45–0.72).

The growth rate in January was over 33% greater compared with November (slopes were significantly different between months, ANCOVA, $P < 0.001$). A nearly identical result was obtained by restricting the ages to a common range for each month (<17 days). The correlation between size-at-age and temperature and zooplankton (ln transformed), for Regions 1–5 over both months was not significant ($r < 0.23$, Table 3).

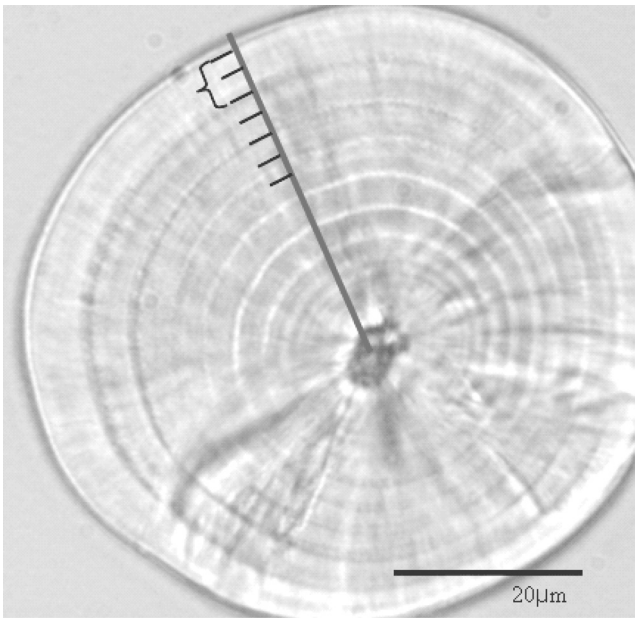

Fig. 4. Image of a 11.6 mm standard length (SL) larval *S. sagax* (10 growth increments), showing, the maximum radius, the location of growth increment widths with the last outer two complete growth increments bracketed.

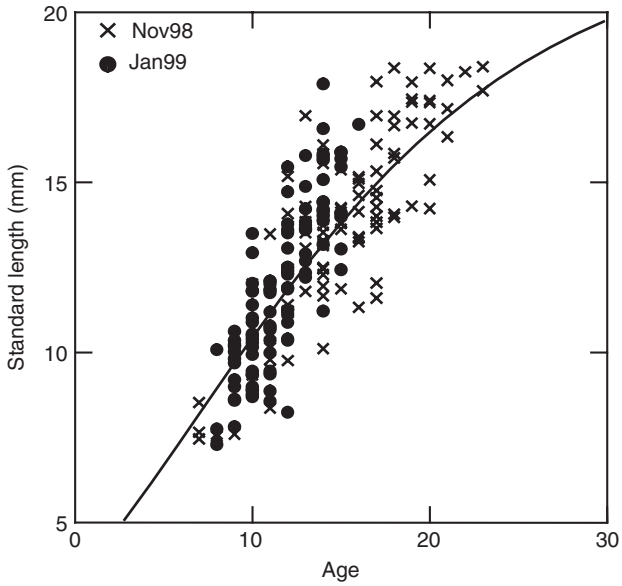

Fig. 5. Standard length (SL) on age (determined as increment count+2) for both cruises. The Laird–Gompertz fit for only November 1998 is shown (Table 2), excluding three outliers.

Table 3. Summary table of ANCOVA and multiple regression models of the dependent variable RG (recent growth) – the back-calculated growth over the previous 2 days before capture – as a function of L_c (standard length at capture, back-calculated to the first complete increment), region, temp (water temperature) and zoopl, micro-zooplankton concentration (in transformation)

The sample size (n) is reduced in November multiple regression model as microzooplankton was only collected in the neuston net. Those variables in bold are statistically significant ($P < 0.05$). Note that temperature is not significantly correlated with recent growth, and zooplankton is positive in November, but negative in January

Month	Regions	Model	n	R^2
November	1, 3, 4	$RG = \mathbf{L_c} + \mathbf{Region} + \mathbf{Region} \times \mathbf{L_c}$	93	0.54
	1, 3, 4	$RG = -7.01 + \mathbf{0.10} \times \mathbf{L_c} + 0.30 \times Temp + \mathbf{0.93} \times \mathbf{ln(Zoopl)}$	50	0.44
January	1, 4, 5	$RG = \mathbf{L_c} + \mathbf{Region} + \mathbf{Region} \times \mathbf{L_c}$	95	0.42
	1, 4, 5	$RG = -0.47 + \mathbf{0.06} \times \mathbf{L_c} + 0.06 \times Temp - \mathbf{0.24} \times \mathbf{ln(Zoopl)}$	95	0.22

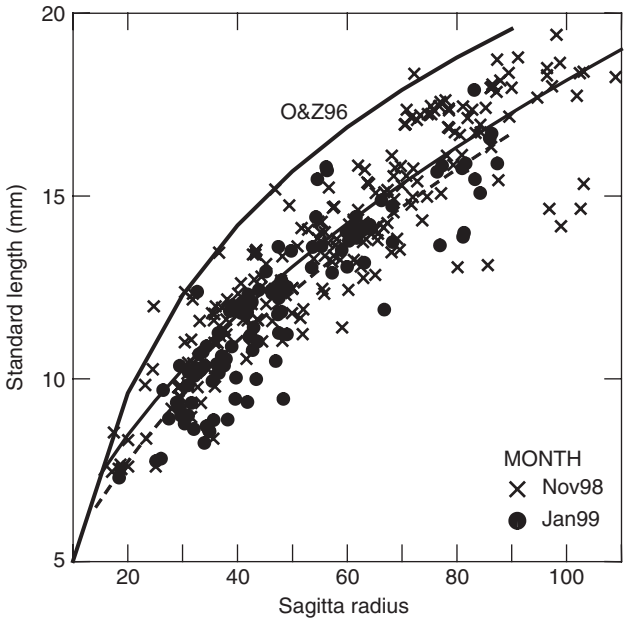

Fig. 6. Non-linear relationship of standard length (SL, mm) on the maximum otolith radius (μm). The curves for the 2 months were slightly, but significantly different. The curve labelled O&Z96 is that for *S. melanosticus*, from Oozeki and Zenitani (1996).

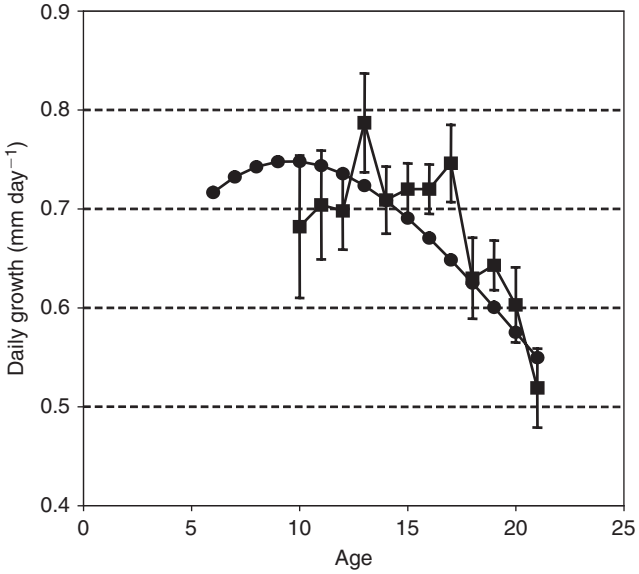

Fig. 7. Estimated growth in mm day^{-1} from the fitted Laird–Gompertz growth equation for November 1998 as a function of larval age (circles), plotted with the back-calculated growth for each daily age class for November 1998 (square symbols, mm day^{-1}, ± standard error).

The larval length–otolith radius relationship (Fig. 6) could be described by the power functions:

$$L = 2.016 \times R^{0.477} \ (r^2 = 0.83, \text{November 1998}),$$

$$L = 1.654 \times R^{0.514} \ (r^2 = 0.80, \text{January 1999}),$$

where L is the SL (mm) and R is the maximum sagittal otolith radius (μm). The two months were significantly different using the linear log–log equivalent form of the power function, with a significantly greater intercept for the November 1998 data (ANCOVA, $P < 0.001$).

To assess our back-calculation, the average daily change in back-calculated SL of the two outer (recent growth, RG) increments ([RG 1 & 2] ÷ 2) for each daily age class was compared with the daily growth independently estimated from November's Laird–Gompertz model (Fig. 7). In general, the two daily growth estimations were similar and declined with age.

As a function of size, the back-calculated growth for Days 1 and 2 pre-capture increased as a function of length or remained constant at approximately 1–2 mm growth (Fig. 8). The growth for previous 2 days before capture exhibited significant differences in the slopes among regions, in both months (ANCOVA, $P < 0.001$, Table 3). In November the slope of the recent growth, as a function of length was significantly greater off Regions 1 and 3 than off the upwelling areas (Regions 4, 5, Table 3, Fig. 8). In January, the slope was also significantly greater at Region 1, than at Regions 4 and 5 (Table 3, Fig. 8). To interpret these differences among regions we compared the explanatory power (R^2 statistic) between the ANCOVA model and a multiple regression model

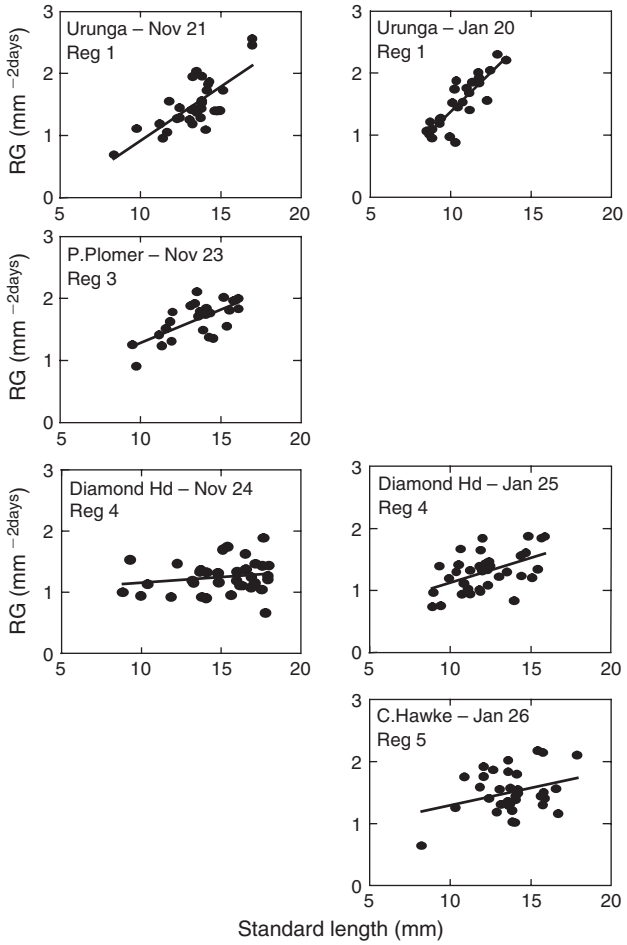

Fig. 8. Back-calculated larval recent growth (RG) over the previous two complete days before capture (mm), as a function of length, back-calculated for the last complete increment, plotted for each region. Left column: November 1998, right column: January 1999.

that did not include Region, but with water temperature and micro-zooplankton concentration. Temperature was not significantly correlated with recent growth in either month, and zooplankton was positive in November, but negative in January (Table 3).

The back-calculated recent growth in SL for Days 1 and 2 pre-capture (RG 1 & 2) was highly correlated with that calculated at Days 3 and 4 pre-capture (Table 4). However, the correlation declined with increasing separation in time, such that RG 1 & 2 was less correlated with RG 7 & 8 (Table 4).

Stable isotope composition and growth rate

There was no significant correlation between $\delta^{13}C$ and length in either month, but there was between $\delta^{15}N$ and length (Fig. 9, $r = 0.47$, 0.52 over all regions in November and January respectively). The overall positive correlation was also apparent within each month and region combination (Fig. 9).

Table 4. The Pearson correlation matrix for the back-calculated recent growth of all larvae for Days 1–2 precapture (RG 1 & 2), Days 3–4 precapture (RG 3 & 4), Days 5–6 precapture (RG 5 & 6) and Days 7–8 (RG 7 & 8)

Interval	RG 1 & 2	RG 3 & 4	RG 5 & 6	RG 7 & 8
RG 1 & 2	1			
RG 3 & 4	0.81**	1		
RG 5 & 6	0.63**	0.74**	1	
RG 7 & 8	0.27*	0.43**	0.66**	1

$n = 105$, $^{**}P < 0.01$, $^{*}P < 0.05$.

The size independent recent growth index (RGI = RG 1 & $2 \div \ln(SL)$) was significantly related to the stable isotope composition in November (Fig. 10*a*, $RGI = 1.488 - 0.104 \times \delta^{15}N$, $n = 69$, $P < 0.001$, $R^2 = 0.29$, Fig. 10*b*, $RGI = 2.300 + 0.096 \times \delta^{13}C$, $n = 70$, $P < 0.001$, $R^2 = 0.21$), such that faster growing pilchard larvae were depleted in $\delta^{15}N$ and enriched in $\delta^{13}C$. There was no significant correlation in January.

In November, pilchard larvae from the pre-upwelled, EAC conditions off Regions 1 and 3 were significantly depleted in $\delta^{15}N$ and enriched in $\delta^{13}C$, compared with those off the upwelling regions (i.e. Region 4, Fig. 11, Tukey's test $P < 0.05$). In January, Region 1 was also significantly depleted in $\delta^{15}N$, while Regions 1 and 5 were significantly depleted in $\delta^{13}C$ compared with Region 4 (Tukey's test, $P < 0.05$). Faster average recent growth for each region (shown as expanding symbols in Fig. 11) was associated with the depleted $\delta^{15}N$ and enriched $\delta^{13}C$ of the pre-upwelled EAC waters.

Discussion

Growth rates in different regions and months

Our yardstick for comparing the significance of upwelling on larval pilchards was the back-calculated growth over the previous two complete daily growth increments before capture. Our back-calculation seems to be a robust measure of recent growth, as shown by the two different back-calculation methods (Watanabe and Kuroki 1997; Vigliola *et al*. 2000), and by the comparison with the daily growth rate from the Laird–Gompertz relationship. A 2-day response in growth (rather than some lag effect) is justified by the documented 2–3 days response of larval menhaden (Maillet and Checkley 1990), and by the declining correlation of RG 1 & 2 with RG 3 & 4, RG 5 & 6 and RG 7 & 8. However, the recent growth rate varied with larval size, such that we had to compare this regression slope among regions. The slope on both cruises was steeper in the northern, pre-upwelled waters of the EAC off the town of Urunga, than the southern upwelled waters off Diamond Head. The decline in slope was a result of the decline in the growth rate of larger pilchards (>10 mm) in upwelled water, rather than an increase in growth of smaller larvae. Thus, contrary to our expectations, we found that

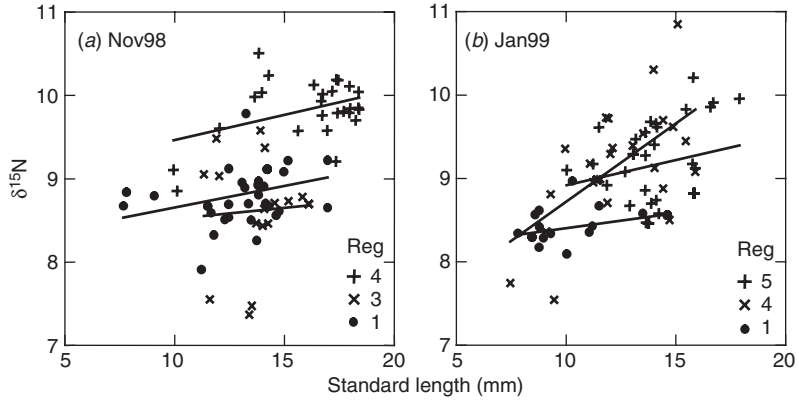

Fig. 9. Scatterplot of the $\delta^{15}N$ on standard length of larval *S. sagax* in (*a*) November 1998 and (*b*) January 1999. Regions (Reg) are labelled with different symbols, with Region 4 experiencing uplifting in November and Regions 4, 5 experience upwelling in January.

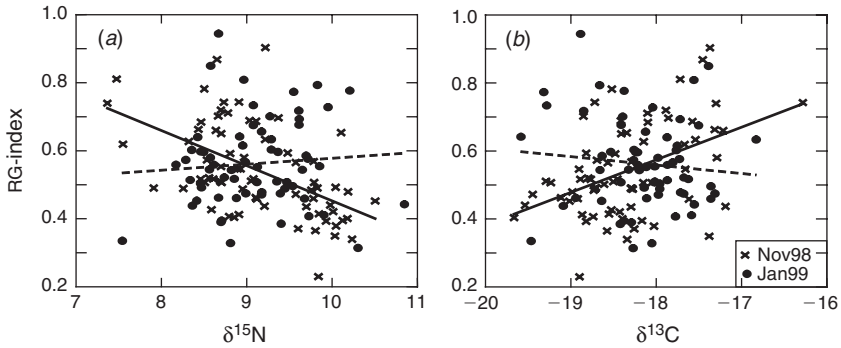

Fig. 10. Recent growth (RG) index (size adjusted) of larval *S. sagax* for November (solid line) and January (dashed line), plotted on (*a*) $\delta^{15}N$ and (*b*) $\delta^{13}C$.

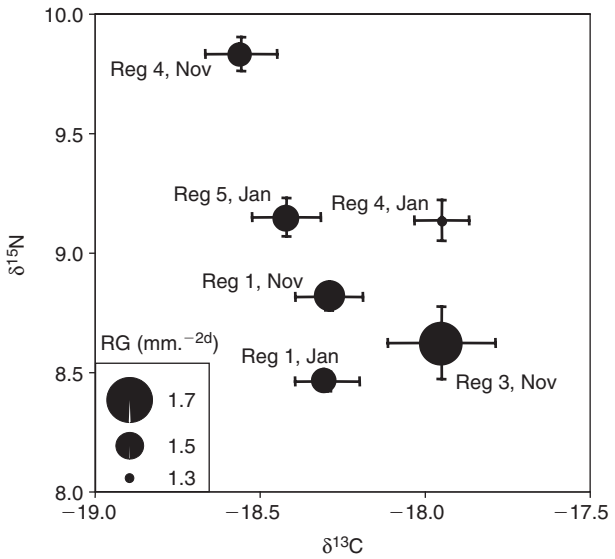

Fig. 11. Average $\delta^{15}N$ and $\delta^{13}C$ (± s.e.) for larval *S. sagax* at each region (Reg) in November 1998 (Nov) and January 1999 (Jan), with the expanding symbols proportional to recent growth over the 2 days before capture.

larger pilchard larvae grew significantly slower during the 2 days before capture in the upwelling regions (Regions 4 and 5), compared with those from the pre-upwelled waters.

A clue to our surprising result may be found in the stable isotope signature, which showed that the slower growing larvae in the upwelled waters were comparatively enriched in $\delta^{15}N$ and depleted in $\delta^{13}C$ relative to those faster growing larvae from Regions 1 and 3 (Urunga and Point Plomer). Therefore, contrary to general expectations (e.g. Ware and Thomson 1991), larval pilchard had a different diet in upwelled conditions that did not stimulate their growth. Nitrate is the hallmark of upwelled waters which are typically enriched in ^{15}N (4–6‰, Altabet and McCarthy 1986; Boutton 1991) and depleted in ^{13}C (Gaston *et al*. 2004), consistent with the stable isotope composition of larvae from Regions 4 and 5.

The upwelled waters were slightly cooler by 0.5–1°C (Syahailatua 2004), but water temperature was not a significant covariate in an expanded regression model of recent growth, for either cruise. Microzooplankton <100 μm abundance was significantly correlated with recent growth in November, but the data were unfortunately incomplete

in November, compared to January when it was negatively correlated. Therefore, the cause of the slower short-term growth is still unclear, and could involve turbulence, disruption of the thermocline by upwelling, or the quality or size structure of zooplankton. The significant regressions of the recent growth index on stable isotope ratios in November, show that the nutrient sources (diets) actually differed among regions and growth rates (rather than a purely physical difference such as turbulence). At the scale of months, the faster growing larvae in January was clearly a result of the 5–6°C warmer water compared to November.

The allometric relationship of fish size-otolith size in the current study was not as marked as found for *S. melanosticus* (Oozeki and Zenitani 1996, Fig. 6). The cause could be because of possible genetic differences among stocks or subspecies, or a result of more rapid growth in the Kuroshio producing proportionally smaller otoliths. The effects of this non-linearity was addressed by Watanabe and Kuroki (1997), who determined a novel non-linear back-calculation of recent growth based on the biological intercept method. We found identical back-calculations between this method and the modified Fry equation (Vigliola *et al*. 2000), which was also consistent with the daily growth expected from the overall Laird–Gompertz growth model. The variance in RG 1 & 2 compared with the growth model (Fig. 7) was in part a result of the unequal representation of larvae, with ages from different regions.

Larval growth and early life history of pilchards

The slower growth of larval pilchard was perplexing, but may be interpreted in the light of Watanabe's (2002) explanation of the pilchard life history in the Kuroshio Extension (equivalent of the EAC's Tasman front). They too found slower growth inshore, but found enhanced growth offshore in the frontal waters of the Kuroshio Extension. Larval pilchards are advected away from the coast by the Kuroshio, where larvae grow and then migrate across the transition region to the northern summer feeding grounds off the island of Hokkaido (Watanabe 2002). Adults then migrate south to spawn off Kyushu and Shikoku.

Slower growth by larval *Sardinops* nearshore was also observed off the coast of California (Logerwell and Smith 2001). The present study used the extensive California Cooperative Fisheries Investigations data set to determine the location of 'survivors' habitat', where patches of $\geq$18 days old larvae were found, which corresponded to sea surface temperature images of mesoscale eddies in offshore regions. *Sardinops* eggs, chlorophyll biomass and zooplankton volume were the greatest inshore.

The lifecycle of the east coast pilchards could mirror that observed for the Kuroshio, with adults migrating north and spawning in coastal areas of northern NSW and southern Queensland in late winter (Ward *et al*. 2003). Eggs and larvae are advected southwards by the EAC, some along the coast, but larval growth and survival is enhanced for those transported past the separation zone and east into the Tasman Front, where they grow and migrate back to the coastal summer feeding grounds near Jervis Bay (southern NSW). The tendency for larger larvae to be found at the southern end of the current study area is consistent with larval transport south, from the northern spawning areas. During our two cruises we did not continue to sample the front out into the Tasman Sea to test this hypothesis, although a recent cruise in September 2004 found pilchard larvae to be abundant and larger in the Tasman Front, east of 153°E and 300 km from eastern Australia (I. M. Suthers, unpublished data).

The parameter estimates for the Laird–Gompertz model (Fig. 5) provide an average growth rate of 0.53 mm day^{-1} (10–25 days old), consistent with those calculated off Japan, California, South Africa, South America (as reviewed in Gaughan *et al*. 2001), but double the larval growth found in the Leeuwin Current (Gaughan *et al*. 2001). It is therefore possible that larval pilchard in the EAC are not food limited, in comparison with those from the Leeuwin Current.

Larval fish ecology of stable isotopes

Larval pilchards increased in δ^{15}N with length, presumably as larvae consumed more higher trophic order plankton. A positive relationship between δ^{15}N and size was demonstrated in larval anchovy (10–30 mm, Lindsay *et al*. 1998) and a negative relationship in larval smallmouth bass (4–15 mm, Vander Zanden *et al*. 1998), as the larvae lose the maternal signature and select larger and isotopically different prey. A weak positive relationship between δ^{13}C and size was reported in both these studies, and was observed in the current study as well. Therefore, the δ^{15}N composition of larval fish can provide an index of assimilation, and contrast of tissue turnover *v.* growth (Vander Zanden *et al*. 1998; Bosley *et al*. 2002), but the general utility is more suited to the pelagic-benthic transition in the early life history (e.g. Herzka *et al*. 2001).

Considerable challenges remain in the use of stable isotopes in marine fish larvae, for the reconstruction of food webs and particularly the calibration of turnover and depuration of stable isotope signatures. The prey species' signatures are unknown, as obtaining sufficient quantities of nauplii or particular copepod species is difficult. Fractionation between diet and tissue composition is now recognised as being diet- and species-specific, making it difficult to relate signatures to pelagic food chains without a laboratory calibration (Bosley *et al*. 2002). For example two typical prey items, a copepod (*Temora*) and cladoceran (*Penillia*) exhibited a strong response in stable isotope composition to upwelling off the NSW coast, particularly in δ^{13}C (S. Rutten, unpublished data). Rearing of larval pilchards, and sampling further out along the Tasman Front is needed to understand the conundrum posed by the present study: what conditions reduced the growth rate of larval pilchards in an upwelling zone?

The relationship between clupeid production and upwelling is not a simple one, and seems to be species- and location-specific.

Acknowledgements

We acknowledge the support of the Australian Research Council, and the National Research Institute of Fisheries Science (NRIFS), Japan. We thank the excellent seamanship of the captain and crew of the R.V. Franklin and the remarkable CSIRO support staff. Richard Piola provided considerable technical expertise during the cruise, Matt Taylor provided laboratory support and Jocelyn Dela Cruz provided the microzooplankton data. Laurent Vigliola kindly assisted with the modified Fry back-calculation. Two anonymous referees greatly improved the manuscript.

References

Altabet, M. A., and McCarthy, J. J. (1986). Vertical patterns in ^{15}N natural abundance in PON from the surface waters of warm-core rings. *Journal of Marine Research* **44**, 185–201.

Bosley, K. L., Witting, D. A., Chambers, R. C., and Wainright, S. C. (2002). Estimating turnover rates of carbon and nitrogen in recently metamorphosed winter flounder *Pseudopleuronectes americanus* with stable isotopes. *Marine Ecology Progress Series* **236**, 233–240.

Boutton, T. W. (1991). Stable carbon isotopic ratios of natural materials: II. Atmospheric, terrestrial, marine and freshwater environments. In 'Carbon Isotope Techniques'. (Eds D. C. Coleman and B. Fry.) pp. 173–185. (Academic Press: San Diego, CA.)

Bunce, A., and Norman, F. I. (2000). Changes in the diet of the Australasian gannet (*Morus serrator*) in response to the 1998 mortality of pilchards (*Sardinops sagax*). *Marine and Freshwater Research* **51**, 349–353. doi:10.1071/MF99133

Campana, S. E., and Jones, C. M. (1992). Analysis of otolith microstructure data. In 'Otolith Microstructure Examination and Analysis'. (Eds D. K. Stevenson and S. E. Campana.) pp. 73–100. (Canadian Special Publication Fisheries and Aquatic Sciences, Department of Fisheries and Oceans: Ottawa.)

Cresswell, G. R. (1994). Nutrient enrichment of the Sydney Continental Shelf. *Australian Journal of Marine and Freshwater Research* **45**, 677–691.

Cury, P., and Roy, C. (1989). Optimal environmental window and pelagic fish recruitment success in upwelling areas. *Canadian Journal of Fisheries and Aquatic Sciences* **46**, 670–680.

Dann, P., Norman, E. I., Cullen, J. M., Neira, E. J., and Chiaradia, A. (2000). Mortality and breeding failure of little penquins, *Eudyptula minor*, in Victoria, 1995–96, following a widespread mortality of pilchard, *Sardinops sagax*. *Marine and Freshwater Research* **51**, 355–362. doi:10.1071/MF99114

Dela-Cruz, J., Ajani, P., Lee, R., Pritchard, T., and Suthers, I. M. (2002). Temporal abundance patterns of the red tide dinoflagellate *Noctiluca scintillans* along the southeast coast of Australia. *Marine Ecology Progress Series* **236**, 75–88.

Dela-Cruz, J., Middleton, J. H., and Suthers, I. M. (2003). Population growth and transport the red tide dinoflagellate, *Noctiluca scintillans*, in the coastal waters off Sydney Australia, using cell diameter as a tracer. *Limnology and Oceanography* **48**, 656–674.

Gaston, T. F., and Suthers, I. M. (2004). Spatial variation in the $\delta^{13}C$ and $\delta^{15}N$ of liver, muscle and bone in a rocky reef planktivorous fish: the relative contribution of sewage. *Journal of Experimental Marine Biology and Ecology* **304**, 17–33. doi:10.1016/J.JEMBE.2003.11.022

Gaston, T. F., Kostoglidis, A., and Suthers, I. M. (2004). The ^{13}C, ^{15}N and ^{34}S signature of a rocky reef planktivorous fish does indicate different coastal discharges of sewage. *Marine and Freshwater Research* **55**, 689–699. doi:10.1071/MF03142

Gaughan, D. J., Fletcher, W. J., and White, K. V. (2001). Growth rate of larval *Sardinops sagax* from ecosystems with different levels of productivity. *Marine Biology* **139**, 831–837. doi:10.1007/S002270100637

Grant, W. S., Clark, A. M., and Bowen, B. W. (1998). Why RFLP analysis of control region sequences failed to resolve sardine (*Sardinops*) biogeography: insights from mitochondrial DNA cytochrome b sequences. *Canadian Journal of Fisheries and Aquatic Sciences* **55**, 2539–2547.

Griffin, D. A., Thompson, P. A., Bax, N. J., Bradford, R. W., and Hallegraeff, G. M. (1997). The 1995 mass mortality of pilchard: no role found for physical or biological oceanographic factors in Australia. *Marine and Freshwater Research* **48**, 27–42.

Hayashi, A., Yamashita, Y., Kawaguchi, K., and Ishii, T. (1989). Rearing method and daily otolith ring of Japanese sardine larvae. *Nippon Suisan Gakkai Shi* **55**, 997–1000.

Herzka, S. Z., and Holt, G. J. (2000). Changes in isotopic composition of red drum (*Sciaenops ocellatus*) larvae in response to dietary shifts: potential applications to settlement studies. *Canadian Journal of Fisheries and Aquatic Sciences* **57**, 137–147. doi:10.1139/CJFAS-57-1-137

Herzka, S. Z., Holt, S. A., and Holt, G. J. (2001). Documenting the settlement history of individual fish larvae using stable isotope ratios: model development and validation. *Journal of Experimental Marine Biology and Ecology* **265**, 49–74. doi:10.1016/S0022-0981(01)00324-0

Lindsay, D. J., Minagawa, M., Mitani, I., and Kawaguchi, K. (1998). Life history of Japanese anchovy, *Engraulis japonicus*, in Sagami Bay: stable isotope analysis. *Monthly Kaiyo* **29**, 418–424. [In Japanese]

Logerwell, E., and Smith, P. E. (2001). Mesoscale eddies and survival of late stage Pacific sardine (*Sardinops sagax*) larvae. *Fisheries Oceanography* **10**, 13–25. doi:10.1046/J.1365-2419.2001.00152.X

Maillet, G. L., and Checkley, D. M. (1990). Effects of starvation on the frequency of formation and width of growth increments in sagittae of laboratory-reared Atlantic menhaden *Brevoortia tyrannus* larvae. *Fishery Bulletin* **88**, 155–165.

Neira, F. J., Miskiewicz, A. G., and Trinski, T. (1998). Larvae of temperate Australian fishes; Laboratory guide for larval fish identification. (University of Western Australian Press: Nedlands.)

Oke, P. R., and Middleton, J. H. (2000). Topographically induced upwelling off eastern Australia. *Journal of Physical Oceanography* **30**, 512–531. doi:10.1175/1520-0485(2000)030<0512:TIUOEA>2.0.CO;2

Oke, P. R., and Middleton, J. H. (2001). Nutrient enrichment off Port Stephens: the role of the East Australian Current. *Continental Shelf Research* **21**, 587–606. doi:10.1016/S0278-4343(00)00127-8

Oozeki, Y., and Zenitani, H. (1996). Factors affecting the recent growth of Japanese sardine larvae (*Sardinops melanosticus*) in the Kuroshio Current. In 'Survival Strategies in Early Life Stages of Marine Resources'. (Eds Y. Watanabe, Y. Yamashita and Y. Oozeki.) pp. 95–105. (AA Balkema: Rotterdam.)

Roughan, M., and Middleton, J. H. (2002). A comparison of observed upwelling mechanisms off the east coast of Australia. *Continental Shelf Research* **22**, 2551–2572. doi:10.1016/S0278-4343(02)00101-2

Santos, A. M. P., Borges, M. F., and Groom, S. (2001). Sardine and horse mackerel recruitment and upwelling off Portugal. *ICES Journal of Marine Science* **58**, 589–596. doi:10.1006/JMSC.2001.1060

Suthers, I. M. (1998). Bigger? Fatter? or is faster growth better? Considerations on condition in larval and juveniles coral-reef fishes. *Australian Journal of Ecology* **23**, 265–273.

Syahailatua, A. (2004). Biological oceanography of larval fish diversity and growth off eastern Australia. Ph.D. Thesis, University of New South Wales, Sydney.

Thresher, R. E., Bruce, B. D., Furlani, D. M., and Gunn, J. S. (1989). Distribution, advection and growth of larvae of the southern temperate gadoid (*Macruronus novaezelandiae*) in Australian coastal waters. *Fishery Bulletin* **87**, 29–48.

Thresher, R. E., Nichols, P. D., Gunn, J. S., Bruce, B. D., and Furlani, D. M. (1992). Seagrass detritus as the basis of a coastal planktonic food chain. *Limnology and Oceanography* **37**, 1754–1758.

Vander Zanden, M. J., Hulshof, M., Ridgway, M. S., and Rasmussen, J. B. (1998). Application of stable isotope techniques to tropic studies of age-0 smallmouth bass. *Transaction of American Fishery Society* **127**, 729–739. doi:10.1577/1548-8659(1998)127<0729:AOSITT>2.0.CO;2

Vigliola, L., Harmelin-Vivien, M., and Meekan, M. G. (2000). Comparison of techniques of back-calculation of growth and settlement marks from the otoliths of three species of *Diplodus* from the Mediterranean Sea. *Canadian Journal of Fisheries and Aquatic Sciences* **57**, 1291–1299. doi:10.1139/CJFAS-57-6-1291

Ware, D. M., and Thomson, R. E. (1991). Link between long-term variability in upwelling and fish production in the Northeast Pacific Ocean. *Canadian Journal of Fisheries and Aquatic Sciences* **48**, 2296–2306.

Ward, T. M., Staunton-Smith, J., Hoyle, S., and Halliday, I. A. (2003). Spawning patterns of four species of predominantly temperate pelagic fishes in the sub-tropical waters of southern Queensland. *Estuarine and Coastal Shelf Science* **56**, 1125–1140. doi:10.1016/S0272-7714(02)00318-9

Watanabe, Y. (2002). Resurgence and decline of the Japanese sardine population. Fishery Science. In 'The Unique Contributions of Early Life Stages'. (Eds L. A. Fuiman and R. G. Werner.) pp. 243–256. (Blackwell: Oxford.)

Watanabe, Y., and Kuroki, T. (1997). Asymptotic growth trajectories of larval sardine (*Sardinops melanostictus*) in coastal waters off western Japan. *Marine Biology* **127**, 369–378. doi:10.1007/S002270050023

Manuscript received 20 August 2004; revised 8 March 2005; and accepted 12 April 2005.